Electronic Supplementary Information

An Single-Atom Fe-N_4 Catalytic Site Mimicking Bifunctional Antioxidative Enzymes for Oxidative Stress Cytoprotection

Wenjie Ma,[‡,a,e] Junjie Mao, [‡,b] Xiaoti Yang,[a,e] Cong Pan,[a,e] Wenxing Chen,[d] Ming Wang,[a,e] Ping Yu,[a,e] Lanqun Mao[*,a,e] and Yadong Li[c]

[a] *Beijing National Laboratory for Molecular Sciences, Key Laboratory of Analytical Chemistry for Living Biosystems, Institute of Chemistry, The Chinese Academy of Sciences (CAS), CAS Research/Education Center for Excellence in Molecule Science, Beijing 100190, China.*

[b] *College of Chemistry and Materials Science, Anhui Normal University, Wuhu 241002, China.*

[c] *Department of Chemistry, Tsinghua University, Beijing 100084, China.*

[d] *Beijing Key Laboratory of Construction Tailorable Advanced Functional Materials and Green Applications, School of Materials Science and Engineering, Beijing Institute of Technology, Beijing 100081, China.*

[e] *University of Chinese Academy of Sciences, Beijing 100049, China.*

Table of Contents

Experimental Section……..……S1
Characterization of Fe-SAs/NC……..……..…S2
EXAFS analysis…….……..……..…S3
Cyclic voltammetry measurements of Fe-SAs/NC…… S4
CAT-like activity of Fe-SAs/NC-based SAzyme……..….S5
Comparison of CAT-like activity between Fe-SAs/NC-based SAzyme and other reported nanozymes…….……S6

‡ These authors contributed equally to this work.

* Corresponding Author. E-mail: lqmao@iccas.ac.cn, Fax: +86-10-62559373.

S1- Experimental Section

1 Chemical Reagent

Iron phthalocyanine (FePc, Alfa Aesar), zinc nitrate hexahydrate (Alfa Aesar), 2-methylimidazole (Acros), methanol (Sinopharm Chemical), N, N-dimethylformamide (Sinopharm Chemical), 30% H_2O_2 (Beijing Chemical Reagents), 5-tert-butoxycarbonyl-5-methyl-1-pyrroline N-oxide (BMPO, Dojindo), ethylenediaminetetraacetic acid disodium salt (EDTA, Sinopharm Chemical), SOD assay kits (Sigma-Aldrich), hypoxanthine (Sigma-Aldrich), xanthine oxidase (Sigma-Aldrich), DCFDA (Sigma-Aldrich), β-lapachone (β-Lap, Abcam) were used without any further purification. Britton–Robinson buffer (BR buffer) was prepared by mixing 0.04 M H_3PO_4, HNO_3, H_3BO_3, and the pH values of the solutions were adjusted by 0.2 M NaOH. Aqueous solutions were all prepared with pure water obtained from a Milli-Q water system (Millipore, 18.2 MΩ cm). Unless stated otherwise, all experiments were carried out at room temperature.

2 Experimental Details

2.1 Materials Synthesis. ZIF-8 and FePc-encapsulated ZIF-8 were prepared at room temperature. In a typical synthesis of FePc encapsulated ZIF-8, $Zn(NO_3)_2{\cdot}6H_2O$ (734.5 mg) and FePc (25 mg) were dissolved in 50 mL methanol in flask A to form a homogeneous solution. 2-Methylimidazole (810.6 mg) was dissolved in 50 mL methanol in flask B. Then, flask A was rapidly poured into flask B and stirred for 24 h at room temperature. The obtained products were washed with methanol for several times and finally dried in vacuum at 70 °C overnight. ZIF-8 without FePc encapsulation was prepared following the same procedure as that employed for the synthesis of FePc-encapsulated ZIF-8.

FeSAs/NC and NC catalysts were obtained via a high-temperature pyrolysis approach. The as-prepared FePc-encapsulated ZIF-8 or pure ZIF-8 precursors were pyrolyzed on a quartz tube in an electric furnace under nitrogen atmosphere at 900 °C for 3 h and cooled down naturally to room temperature. The obtained Fe-SAs/NC was treated with 0.5 M H_2SO_4 for 24 h and washed several times with distilled water, and finally dried in vacuum at 70 °C overnight.

2.2 Instrument and Characterization. X-ray powder diffraction (XRD) patterns were performed on a Rigaku RU-200b X-ray powder diffractometer with Cu Kα radiation (λ = 1.5406 Å). TEM images were conducted on a Hitachi H-800 transmission electron microscope. High-resolution TEM images were obtained by using a FEI Tecnai G2 F20 S-Twin high-resolution transmission electron microscope operated at 200kV. The high-angle annular dark-field scanning transmission electron microscopy (HAADF-STEM) images were carried out by a Titan 80-300 scanning/transmission electron microscope operated at 300 kV, equipped with a probe spherical aberration corrector.

2.3 XAFS measurements. The X-ray absorption fine structure spectra (Fe K-edge) were collected at 1W1B station in Beijing Synchrotron Radiation Facility (BSRF). The storage rings of BSRF were

operated at 2.5 GeV with a maximum current of 250 mA. Using Si(111) double-crystal monochromator, the data was collected in transmission mode using ionization chamber for Fe foil, FeO, Fe_2O_3, and in fluorescence excitation mode using a Lytle detector for Fe-SAs/NC. All spectra were collected under ambient conditions.

2.4 XAFS Analysis. The obtained EXAFS data were processed according to the standard procedures using the ATHENA module implemented in the IFEFFIT software packages. The k^3-weighted EXAFS spectra were acquired by subtracting the post-edge background from the overall absorption and then normalizing with respect to the edge-jump step. Subsequently, k^3-weighted χ(k) data of Fe K-edge were Fourier transformed to real (R) space using a hanning windows (dk=1.0 $Å^{-1}$) to separate the EXAFS contributions from different coordination shells. To obtain the quantitative structural parameters around central atoms, least-squares curve parameter fitting was conducted using the ARTEMIS module of IFEFFIT software packages. The following EXAFS equation was used:

$$\chi(k) = \sum_j \frac{N_j S_0^2 F_j(k)}{kR_j^2} exp[-2k^2\sigma_j^2] exp[\frac{-2R_j}{\lambda(k)}] \sin[2kR_j + \phi_j(k)]$$

S_0^2 is the amplitude reduction factor, $F_j(k)$ is the effective curved-wave backscattering amplitude, N_j is the number of neighbors in the j^{th} atomic shell, R_j is the distance between the X-ray absorbing central atom and the atoms in the j^{th} atomic shell (backscatterer), λ is the mean free path in Å, $\phi_j(k)$ is the phase shift (including the phase shift for each shell and the total central atom phase shift), σ_j is the Debye-Waller parameter of the j^{th} atomic shell (variation of distances around the average R_j). The functions $F_j(k)$, λ and $\phi_j(k)$ were calculated with the ab initio code FEFF8.2.

2.5 Cyclic voltammetry. Cyclic voltammetry measurements were performed on a computer-controlled electrochemical analyzer (CHI 730D, Shanghai, China), with an Ag/AgCl (KCl, 3 M) electrode as reference electrode and a Pt wire as counter electrode. For the preparation of working electrodes, 1 mg of Fe-SAs/NC or NC catalyst was dispersed into 1 mL of pure water under sonication for 1 h. Then, 10 μL of the suspension was drop-coated onto glassy carbon (GC) electrode (3 mm in diameter). The electrode was dried under ambient conditions, followed by dropwise coating of 0.5% Nafion (2 μL). The prepared working electrodes were used for cyclic voltammetric measurements.

2.6 Catalase-like activity of Fe-SAs/NC. The CAT-like activity was verified by determining the O_2 generation during H_2O_2 decomposition using a portable dissolved oxygen meter (Seven2Go™ DO, Mettler Toledo). In a typical test, 5 μg/mL Fe-SAs/NC was added to a solution of 5 mM H_2O_2 in BR buffer solution (pH 7.0), and the generated O_2 solubility (unit: mg/L) was recorded at different reaction times. The kinetic analysis of the Fe-SAs/NC with H_2O_2 as the substrate was performed by varying the concentration of H_2O_2 (0.5-4.0 mM) in the presence of Fe-SAs/NC at fixed concentration of 5 μg/mL. The corresponding Lineweaver-Burk plots were obtained from Michaelis-Menten curves. For comparison, the CAT-like activity of NC was also conducted under

identical conditions. In order to compare the efficiency of Fe-SAs/NC with other reported nanozymes, we calculated the TOF (turnover frequency) values per active site of Fe-SAs/NC-based enzyme and nanozymes reported in literature, according to the following equation and the results were summarized in Table S2:

$$TOF = V_{max}/C_{active\ sites}$$

where, V_{max} represents the maximum rate achieved by the system, at saturating substrate concentration. $C_{active\ sites}$ stands for the concentration of active sites in the system.

2.7 SOD-like activity of Fe-SAs/NC. The ability of Fe-SAs/NC to scavenge superoxide and its comparison with NC was determined using SOD assay kits following the manufacturer's instructions.

2.8 Electron paramagnetic resonance (EPR) spectroscopy. EPR measurement were conducted using a Brucker model EPR 300E spectrometer, which was equipped with a Quanta-Ray Nd:YAG laser (532 nm). For all EPR measurements, the same quartz capillary tube was used to minimize experimental errors. In a typical measurement, 50 μg/mL Fe-SAs/NC or NC was added to a mixture of 25 mM BMPO, 0.2 mM EDTA, 0.5 mM hypoxanthine and 0.05 U/mL XO in BR buffer solution (pH 7.0). EPR spectrum was recorded after 1.5 min of mixing.

2.9 Cell culture. HeLa cells were purchased from (National Infrastructure of Cell Line Resource, China) and maintained in high-glucose dulbecco's modified eagle medium (DMEM) supplemented with 10% fetal bovine serum (FBS) and 1% penicillin/streptomycin at 37 ^{0}C in the presence of 5 % CO_2. For the intracellular delivery, cells were sub-cultured and seeded in 48-well plates 24 h prior to experiment. DMEM, FBS and penicillin/streptomycin were purchased from Gibco (NY, USA).

2.10 Cell uptake study of Fe-SAs/NC-based SAzyme. To study the cellular uptake of Fe-SAs/NC-based SAzyme, HeLa cells were seeded at a density of 1.5×10^{-5} cells in glass bottom cell culture dish (NEST Biotechnology, Wuxi, China) for 24 h prior to experiment, and then treated with Fe-SAs/NC-based SAzyme (at a concentration of 30 μg/mL) for 12 h at 37 °C. At the end of incubation, the cells were washed thoroughly with Dulbecco's phosphate-buffered saline (DPBS) twice, followed by confocal laser scanning microscopy (CLSM) imaging on OLYMPUS FV1000-IX81.

2.11 Intracellular ROS detection of cells. The intracellular ROS levels of HeLa cells with and without Fe-SAs/NC-based SAzyme treatment were measured using 2',7'-dichloro-dihydrofluorescein diacetate (DCFDA-H_2) staining and flow cytometry analysis. HeLa cells were seeded in a 24-well plate at a density of 5×10^4 per well, with 12 h of Fe-SAs/NC-based SAzyme treatment, the cell culture medium was replaced and then treated with β-Lap for 6 h. At the end of incubation, the cells were harvested and washed with DPBS, followed by DCFDA (1 μM) staining, and immediately subjected to flow cytometry analysis on a Beckman Coulter CytoFLEX (Beckman Coulter, USA). Control experiments using NC nanoparticles were carried out in the same procedure to that of using Fe-SAs/NC-based SAzyme.

2.12 Cell viability of HeLa cells with Fe-SAs/NC and β-Lap co-treatment. To verify Fe-

SAs/NC-based SAzyme can protect cells against oxidative stress, HeLa cells were seeded in 48-well plates at a density of 2.5×10^{-4} cells per well for 24 h prior to experiment. At the day of experiment, Fe-SAs/NC-based SAzyme were added to cells at the final concentration ranging from 30 to 50 μg/mL. After 12 h of incubation, the mixtures were replaced with fresh cell culture medium, followed by 12 h of 10 μM β-Lap treatment, and then cell viability was assayed by using Alamar-Blue assay. Control experiments using NC nanoparticles were studied under the same condition to that of Fe-SAs/NC nanocomposites.

S2-Characterization of Fe-SAs/NC

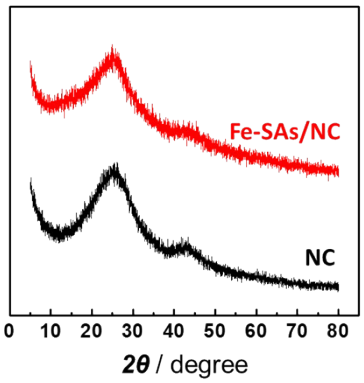

Fig. S1 PXRD patterns of the NC (black line) and Fe-SAs/NC (red line).

S3- EXAFS analysis

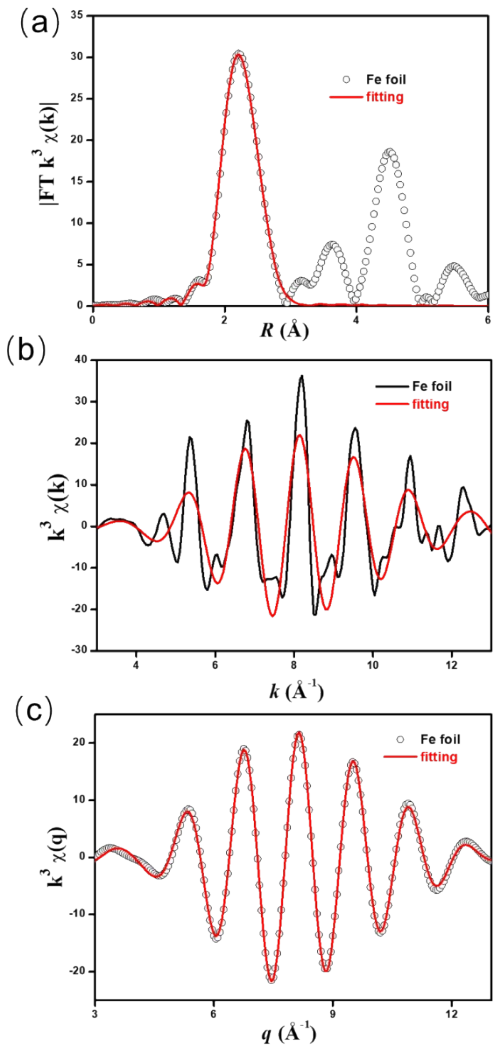

Fig. S2 The corresponding EXAFS fitting curves of Fe foil at(a) R space, (b) k space and (c) q space.

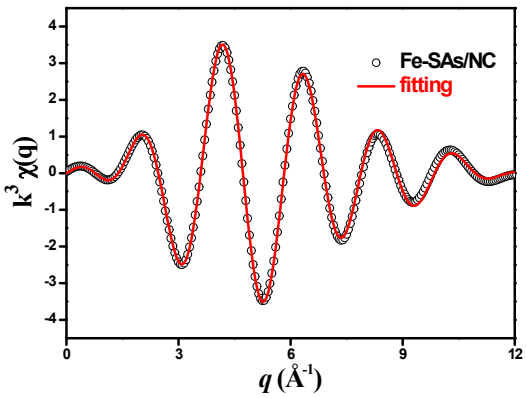

Fig. S3 The corresponding EXAFS fitting curves of Fe-SAs/NC at q space.

Table S1. Structural parameters extracted from the Fe K-edge EXAFS fitting. (S_0^2=0.74)

sample	Scattering pair	CN	R(Å)	$\sigma^2(10^{-3}Å^2)$	ΔE_0(eV)	R factor
Fe-SAs/NC	Fe-N	4.2	2.01	7.3	-2.2	0.002
Fe foil	Fe-Fe1	8*	2.46	4.9	4.5	0.005
	Fe-Fe2	6*	2.84	5.4		

S_0^2 is the amplitude reduction factor; CN is the coordination number; R is interatomic distance (the bond length between central atoms and surrounding coordination atoms); σ^2 is Debye-Waller factor (a measure of thermal and static disorder in absorber-scatterer distances); ΔE_0 is edge-energy shift (the difference between the zero kinetic energy value of the sample and that of the theoretical model). R factor is used to value the goodness of the fitting.

* This value was fixed during EXAFS fitting, based on the known structure.

Error bounds that characterize the structural parameters obtained by EXAFS spectroscopy were estimated as N ± 20%; R ± 1%; σ^2 ± 20%; ΔE_0 ± 20%.

Fe-SAs/NC (FT range: 2.0-11.0 $Å^{-1}$; fitting range: 0.7-2.0 Å)

Fe foil (FT range: 2.0-12.5 $Å^{-1}$; fitting range: 1.3-3.0 Å)

S4- Cyclic voltammetry of Fe-SAs/NC

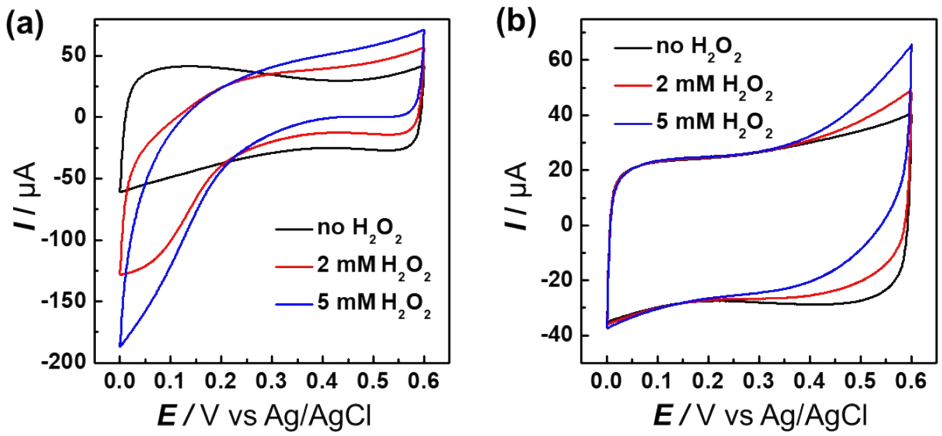

Fig. S4 Typical cyclic voltammograms obtained at Fe-SAs/NC- (a) and NC-modified (b) glassy carbon (GC) electrodes in the absence (black line) and presence of H_2O_2 (red line for 2 mM, blue line for 5 mM) in B-R buffer (pH 7.0) saturated with N_2.

The capability of Fe-SAs/NC to mimic CAT was studied by using cyclic voltammetry with Fe-SAs/NC-modified glassy carbon (GC) electrode as a working electrode in Britton-Robinson (B-R) buffer (pH 7.0) (Figure S4a). For comparison, cyclic voltammetry with the NC-modified GC electrode was also recorded under the same condition (Figure S4b). No redox peaks were recorded at the Fe-SAs/NC-modified GC electrode in BR buffer solution in the absence of H_2O_2, possibly because of the large background current resulted from the porous and conducting NC. The addition of H_2O_2 into the solution produces anodic current commencing at ca. +0.23 V and cathodic current starting at ca. +0.21 V, which were ascribed to oxidation and reduction of H_2O_2, respectively. However, at the NC-modified electrode, the addition of H_2O_2 did not produce current response at the potentials close to those at the Fe-SAs/NC-modified GC electrode. These results indicate that the Fe-SAs/NC can catalyze both the oxidation and reduction of H_2O_2, i.e., disproportionation of H_2O_2, and thus mimic CAT.

S5- CAT-like activity of Fe-SAs/NC-based SAzyme

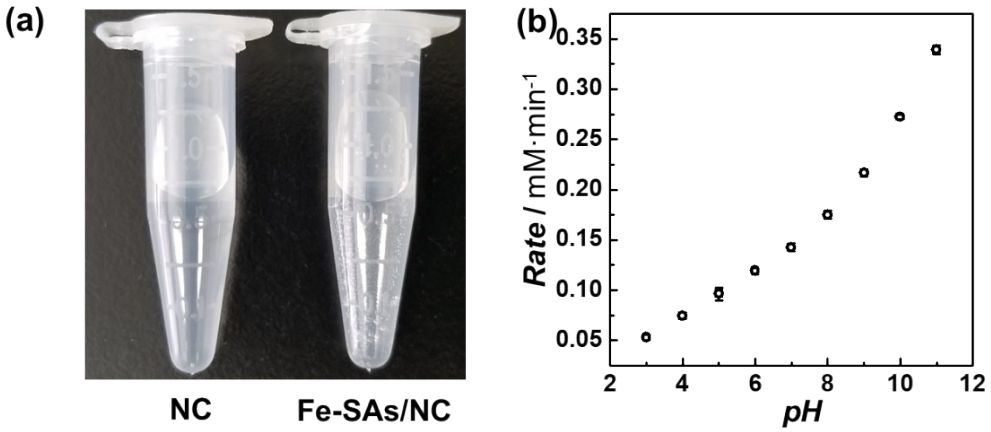

Fig. S5 (a) Images of systems in BR buffer solution (pH 7.0) containing 5 mM H_2O_2 catalyzed by NC (left) and Fe-SAs/NC (right) catalysts for 5 min. (b) Effect of pH on the catalytic activity of Fe-SAs/NC catalysts.

S6- Comparison of CAT-like activity between Fe-SAs/NC-based SAzyme and other reported nanozymes.

Table S2. TOF values per active site of Fe-SAs/NC-based enzyme with other reported nanozymes.

Catalysts	*Vmax*/mM·min^{-1}	Metal content/wt%	$C_{Catalysts}$/μg·mL^{-1}	TOF/min^{-1}	Reference
Fe-SAs/NC	0.405	0.25%*	5	1809.34	This work
Co_3O_4 nanoplates	0.143	73.4%	20	0.57	ACS Appl. Mater. Interfaces 2014, 6, 7090-7098
Co_3O_4 nanorods	0.113	73.4%	20	0.45	
Co_3O_4 nanocubes	0.074	73.4%	20	0.30	
Pd octahedrons	0.354	100%	25	1.51	ACS Nano 2016, 10, 10436-10445
Mn_3O_4 nanoflowers	7.33	72%	5	111.86	Angew. Chem. Int. Ed. 2017, 56, 14267-14271

* The Fe content is about 0.25 wt%, measured by inductively coupled plasma optical emission spectrometry (ICP-OES) analysis.